Digital Twin of Electric Drivetrain: Approach for Virtual Validation of Different Load Profiles

Muhammad Azeem
Department ESME, Ghent University
Flanders Make@UGent - MIRO
Ghent, Belgium
Muhammad.Azeem@ugent.be

Mehmet Güleç
Department ESME, Ghent University
Flanders Make@UGent - MIRO
Ghent, Belgium
Mehmet.Gulec@ugent.be

Peter Sergeant
Department ESME, Ghent University
Flanders Make@UGent - MIRO
Ghent, Belgium
Peter.Sergeant@ugent.be

Karel Vanthuyne
Department ESME, Ghent University
Flanders Make@UGent - MIRO
Ghent, Belgium
Karel.Vanthuyne@ugent.be

Simon Vanpaemel
Dept. Mechanical Engineering, KU Leuven
Flanders Make@KU Leuven
Leuven, Belgium
simon.vanpaemel@kuleuven.be

Mohamed Amine Frikha
Vrije Universiteit Brussel
Flanders Make@VUB - MOBI
Brussels, Belgium
Mohamed.Amine.Frikha@vub.be

Xiao Ma
Flanders Make CoDesignS
Leuven, Belgium
xiao.ma@flandersmake.be

Niels Divens
Flanders Make MotionS
Leuven, Belgium
niels.divens@flandersmake.be

Mohamed El Baghdadi
Flanders Make@VUB - MOBI
Brussels, Belgium
Mohamed.El.Baghdadi@vub.be

***Abstract*—When an electric drivetrain is ordered for deployment under load conditions different from those encountered during its design and testing phases, it is crucial to evaluate its performance beforehand. However, the experimental validation of the efficiency of an electric drivetrain for a new load profile is time-consuming and costly. This article proposes a digital twin approach to estimate the efficiency of an entire drivetrain for a new load profile—one that has not yet been tested on the physical asset. The parameters of the digital twin are determined through a system-level optimization study, utilizing measured data from the load cycles in the time domain. Utilizing this digital twin, the efficiency of the drivetrain is estimated for a new load profile. Subsequently, experimental validation is conducted. The results demonstrate that the proposed approach is accurately assessing drivetrain performance in terms of efficiency for new load profiles, facilitating informed decision-making in deployment scenarios.**

Keywords— digital twin, drivetrain, power electronics, permanent magnet motor, gearbox, validation

I. Introduction

Industry 5.0 launches several terminologies into our world in terms of artificial intelligence, cyber-physical systems, the internet of things, and so on. All those terms briefly aim to achieve more intelligent, efficient and communicative systems. Nowadays virtual validation is one of the hottest topics in the industry and academia. Virtual validation aims to understand the performances of a product without doing any tests, which is very important for the industry to avoid costly and tedious experiments at all for new scenarios [1].

A digital twin of a product is essential to perform a virtual validation. A digital twin is a digitalized model of a product, which can be developed from pure physics based models to metamodels, and is fed by field data from the existing products. Digital twin technology has been applied to various fields; however, there is limited literature available on its application in the field of electric drivetrains. In electric drivetrains, digital twins are primarily utilized for parameter estimation in motor control and condition monitoring, with the goals of fault diagnosis and smart maintenance [2-3]. Rassõlkin [4] proposed a digital twin of an electric motor based on an empirical model to estimate the performance of the electric propulsion. Rodríguez et al. studied a digital twin of an electric drivetrain to predict the thermal behaviour of an inverter [5]. In [6], a digital twin for three phase inverter-driven permanent magnet (PM) motors is investigated in terms of parameter estimation. However, these studies have limitations such as: 1) The digital twin and parameter identification were carried out only for an individual drivetrain component, such as the motor. A holistic digital twin representing the entire drivetrain, comprising components like power electronics, motor, gearbox, and load motor, is lacking. 2) The motor's digital twin parameters were obtained by fitting on a limited number of load data points, rather than the full drive cycle data to take into account all dynamic behaviour. 3) Furthermore, to the author's knowledge, the virtual validation of the efficiency of an electric drivetrain for new load profiles has not been performed in literature. It is crucial to understand how these drivetrains will perform under different load cycles for which no experimental data are available.

In this study, a digital twin of a complete drivetrain is developed to virtually validate efficiency for new load profiles. The key contributions of this article are as follows:

1. A digital twin of a complete electric drivetrain is developed, encompassing power electronics, motor, gearbox, and load. This also integrates the dynamics and interactions among its components.
2. By employing the digital twin, the efficiency of new load profile is estimated and also validated through experiments.
3. The digital twin is developed on simple, readily available output and input data from the drivetrain, with no need for additional sensor data.

II. Approach for Virtual Validation

A. Drivetrain topology for which validation is needed

The electric drivetrain consists of a power electronic converter, cable, electric motor (permanent magnet synchronous machine), gearbox and load: see Fig. 1. This is a typical drivetrain for many applications in industry or automotive.

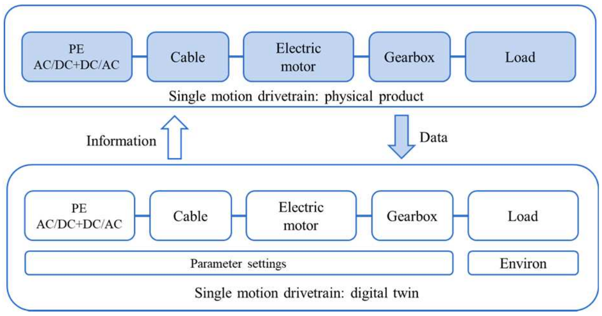

Fig. 1. Topology of the considered electric drivetrain

The details of the test setups for these drivetrains will be given in section V.

B. Conventional approach for validation

When a new electric drivetrain is designed for a given application, the typical approach for validation is shown in Fig. 2. The physical products are called "motion products" (MP), which are sold at customers and which operate "in the field" e.g. at their premises or on the road in case of vehicles. We discuss the approach in Fig. 2 in detail. In the design phase, typically models are made to simulate the performance of the drivetrain. When the designer is satisfied with the simulated results, a physical validation is done: a prototype is built and tested on a test rig in a laboratory. As the testing is on a laboratory setup, a lot of detailed and accurate data is typically collected: torque and speed waveforms, current and voltage waveforms, temperatures… If the physical validation reveals shortcomings, the design is updated.

Then, mass production is started: this is the right part of Fig. 2. These motion products are "in the field", and the quality of available data is typically lower because not all quantities are measured. In the conventional approach, these field data are not used to improve the model (feedback arrow in dashed line).

Also, in this conventional approach, drivetrain performance is typically simulated using models based on datasheet values. However, these models do not accurately reflect real system behavior at the full system level, as we will show in Section VI.

More importantly, if a new load profile is needed for which no data are available, this conventional approach requires a new physical test campaign for this new load profile.

C. Virtual validation approach

The idea in this paper is to use many available data sets on the many drivetrains in the field to develop a digital twin, in order to predict the efficiency of the drivetrain for non-tested load profile.

This approach has two advantages: first, there is no need to do additional measurements on the lab setup; second, the variations that occur in the "identical" products in the field, are automatically taken into account. In this paper, we limit ourselves to 1 motion product A1 (MP-A1), but the approach is valid for *n* products.

The approach is shown in Fig. 3, and is explained in detail based on this figure. We start from a model of the drivetrain, containing several parameters.

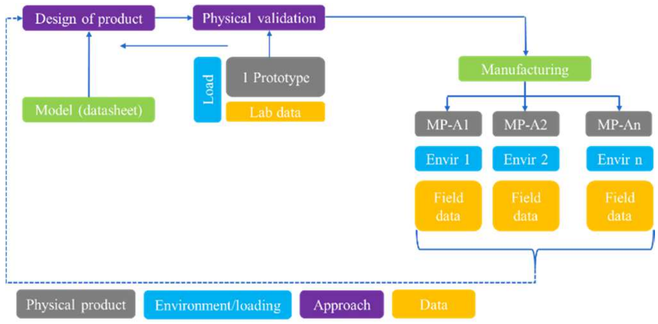

Fig. 2. Conventional approach for validation, and manufacturing of many motion products (MP) that run in the field.

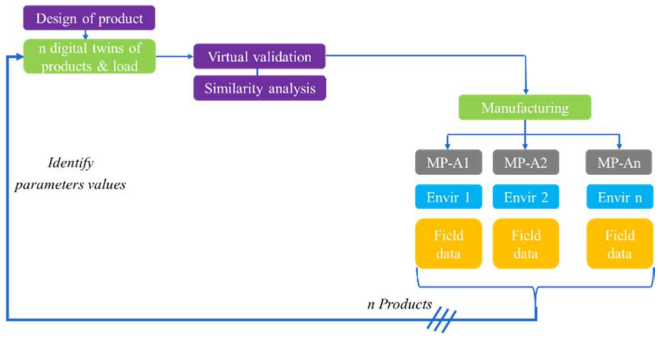

Fig. 3. Virtual validation approach.

The identification of the parameters' values is done based on MP-A1 measurement data in different environmental conditions, and the result is a digital twin. The model details are given in section III.

Next, the virtual validation is done for a new load profile. The virtual validation means running the digital twin for new load cycle, resulting in a computed output that takes into account the information obtained from product in the field. In this paper, we choose the average efficiency over a drive cycle of a vehicle as output quantity. If the drivetrain efficiency for the new load profile meets the requirement, manufacturing can commence (arrow from virtual validation to manufacturing).

It is worth noting that data from the *n* products in the field can now also be used to enhance the alignment between digital twin predictions and experimental data. This gives *n* digital twins, one for each physical product. The *n* digital twins can be merged into one "fleet digital twin", but in this paper, we consider just one physical product (MP-A1).

III. Component Models of the Drivetrain

This section covers the drivetrain model, which consists of component models for power electronics, electric motor and gearbox. The drivetrain scheme is displayed in Fig. 4 and

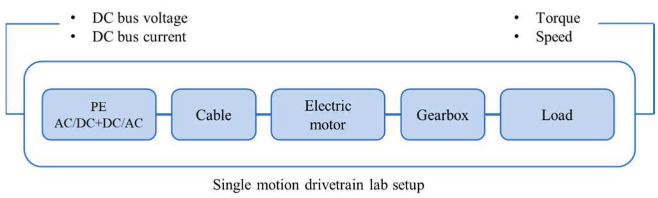

Fig. 4. Components in the drivetrain model, and measured quantities used for the identification of the parameters.

shows measured quantities which can be used for identification of the parameters. The following subsections provide the details about the component models and the parameters.

A. Model of the power electronics

This part focuses on the modelling of the bidirectional two-level three-phase voltage source inverter using an analytical approach. The equivalent circuit of the IGBT power inverter is illustrated in Fig. 5.

The modeling of the traction inverter will emphasize a half-bridge layout to facilitate the formulation process. It is possible to analyze the performance of IGBT switches and their anti-parallel diodes during conducting and non-conducting states through the use of the equivalent circuits of the power modules. This will be achieved through equivalent circuits utilizing the DC voltage to characterize the on-state voltage drop and a resistor to account for conduction losses.

The average signal model is employed to achieve a rapid simulation, leveraging the benefits of the analytical model. Fig. 6 illustrates the use of the average signal model in the context of sinusoidal PWM (SPWM) modulation technique.

The digital twin proposed in this study serves as a platform for evaluating efficiency of the power converter. Consequently, it is critical to include power converter losses in the modelling process. The following section details the calculation of these losses. The dissipation of the IGBT power module primarily includes conduction loss P_{cond} and switching loss P_{sw}. The average power loss of the IGBT is expressed as follows:

$$P_{IGBT} = P_{cond} + P_{sw} \tag{1}$$

The loss in the anti-parallel diode is determined by both the forward conduction loss and reverse recovery loss P_{rec} as:

$$P_{\text{Diode}} = P'_{\text{cond}} + P_{\text{rec}} \tag{2}$$

To simplify the model, threshold voltage drop, on-resistance, and switching energy loss are considered temperature-independent in the following formulation. The conduction losses for the IGBT and the anti-parallel diode are calculated as the product of the current I_{p} flowing through the collector or anode and the saturation voltage (on-state voltage) over the conducting period. The conduction loss can be expressed as:

$$P_{\text{cond}} = \frac{1}{2}\left(\frac{V_{\text{eq}} I_{\text{p}}}{\pi} + \frac{R_{\text{eq}} {I_p}^2}{4}\right) \tag{3}$$

where V_{eq} is the equivalent voltage drop of the IGBT and diode and R_{eq} is the equivalent on-resistance. The switching loss is formulated as:

$$P_{\text{sw}} = E_{\text{eq}} f_{\text{sw}} \tag{4}$$

where E_{eq} represents the equivalent switching energy of the IGBT (ON and OFF switching) and diode blocking energy, and f_{sw} is the switching frequency of the inverter in hertz.

Summing all losses yields to the final loss formulation as:

$$P_{loss} = k_1 N_r + k_2\, I_p + k_3 I_p^2 + k_4 N_r I_p \tag{5}$$

Where k_1, k_2, k_3, and k_4 are the switching loss factor, voltage drop factor, on-resistance factor, and dynamics factor, respectively, and N_r representing the rotor speed.

B. Model of the electric motor

This section describes the modeling of the electric motor, which is permanent magnet synchronous motor (PMSM) having interior (embedded) magnets.

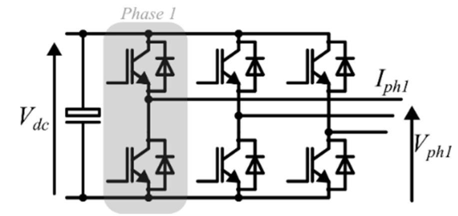

Fig. 5. Equivalent circuit of IGBT-based power inverter.

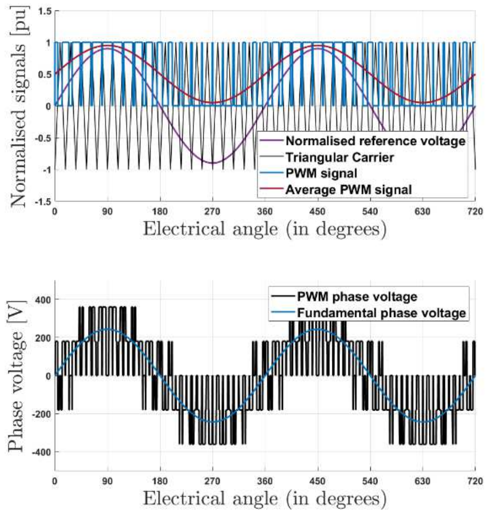

Fig. 6. PWM phase voltage using SPWM technique.

The dynamic model of PMSM can be given in a *dq*-rotor reference frame as:

$$v_q = R_s i_q + L_q \frac{\mathrm{d}i_q}{\mathrm{d}t} + \omega_e L_d i_d + \omega_e \lambda_{\text{PM}} \tag{6}$$

$$v_d = R_s i_d + L_d \frac{\mathrm{d}i_d}{\mathrm{d}t} - \omega_e L_q i_q \tag{7}$$

where v_{d} and v_{q}, i_{d} and i_{q}, and L_{d} and L_{q} are *d*-axis and *q*-axis components of voltage, current, and inductance, respectively. λ_{PM} depicts the flux-linkage of the permanent magnets. R_{s} is the stator resistance, and ω_{e} is the electrical angular speed.

The electromagnetic torque T_{e} of the PMSM consists of the reluctance torque and the magnet torque:

$$T_{\text{e}} = 1.5 p i_{\text{q}}\left(\lambda_{\text{PM}} + \left(L_{\text{d}} - L_{\text{q}}\right) i_{\text{d}}\right) \tag{8}$$

The iron loss is, according to Bertotti's formula, expressed as a function of frequency (f) and maximum flux density (B_{m}), as presented in (9). Here, k_{h}, k_{c} and k_{e}, are the coefficients in the three terms in (9), representing hysteresis, eddy current and excess coefficients, respectively. For the simplicity of the digital twin creation, k_{e} is used as 0.1 [7]. The copper loss of the motor is given by (10).

$$p_{\text{iron}} = k_h f {B_m}^2 + k_c f^2 {B_m}^2 + k_c f^{1.5} {B_m}^{1.5} \tag{9}$$

$$p_c = 3 I^2 R_s \tag{10}$$

The total motor losses can be determined by summing the contributions from (9) and (10). The motor efficiency is then defined as the ratio of mechanical output power p_{out} to electrical input power p_{in}.

$$\eta = \frac{p_{\text{out}}}{p_{\text{in}}} = \frac{p_{\text{in}} - p_{\text{loss}}}{p_{\text{in}}} \tag{11}$$

C. Model of the gearbox

The efficiency of the gearbox is modelled through a power loss model that considers the churning, meshing, rolling, sliding, drag, sealing, and belt losses. This model is coupled with a lumped thermal model to predict the temperature and update the oil viscosity.

The losses of the gearbox and belt assembly can be defined as Eq. (12) where p_{loss} represents the total power loss of the gearbox and belt assembly:

$$p_{\text{loss}} = p_{\text{mesh}} + p_{\text{churn}} + p_{\text{bearing}} + p_{\text{seal}} + p_{\text{belt}} \tag{12}$$

In (12), p_{mesh} represents the load-dependent losses due to the frictional losses in the gear pair [8] and can be a function of friction coefficient, f, load, velocity, and geometry:

$$p_{\text{mesh}} = f(f, load, velocity, geometry) \tag{13}$$

where the friction coefficient can be calculated using Benedict and Kelley's empirical equation [8]:

$$f = \alpha_1 \, log_{10}\left(\frac{\alpha_2 F_{nu}}{\rho \nu V_g U^2}\right) \tag{14}$$

in which F_{nu}, V_g, U, ρ, ν are sliding velocity, sum of the rolling velocities, lubricant density, kinematic viscosity, and normal load per unit length, respectively. Additionally, α_1 and α_2 are model parameters. p_{churn} is the load-independent losses which arises in the partial oil immersion conditions [9]:

$$p_{\text{churn}} = f(\omega, \rho, \nu, Re, Fr, geometry, oil\ level, \beta) \tag{15}$$

where ω, Re, Fr, β are the rotational speed, Reynolds number, Froude number, and model constant, respectively. The bearing-related effects can be divided into rolling p_{rolling}, sliding p_{sliding}, and drag p_{drag} losses:

$$p_{\text{bearings}} = p_{\text{rolling}} + p_{\text{sliding}} + p_{\text{drag}} \tag{16}$$

This model computes all the bearing related losses using the equations and tables provided by [10] and [11]. Finally, p_{seal} and p_{belt} represent the seal and belt-related power losses. In this paper p_{seal} is assumed to be independent of load and rotational speed. Additionally, a viscous friction model is used to model the belt-pully losses.

As the power loss is related to the viscosity and, consequently temperature (Fig. 7), a lumped parameter thermal model is used to predict the temperature:

$$mc_{\text{p,eq}} \Delta\dot{\theta}_{\text{sump}}(t) = -\hbar A_{\text{eq}} \Delta\theta_{\text{sump}} + p_{\text{loss}} \tag{17}$$

where $mc_{\text{p,eq}}$ is the equivalent heat capacity including the gears, bearings, shafts, and oil. Additionally, $\Delta\theta_{\text{sump}} = \theta_{\text{sump}} - \theta_{\infty}$ and $\hbar A_{\text{eq}}$ are the difference between the sump and ambient temperature and the equivalent heat transfer coefficient, respectively. Detailed information about gearbox modeling and identification can be found in [12].

IV. Digital Twin of the Drivetrain

The model of the complete drivetrain is called digital twin if the identification of parameters is done using measured data of one physical asset. Therefore, the component models of section III need identification of the parameter values. This identification procedure is explained in this section. In this paper, the identification is done one time with several load cycles for a given product, but a further extension can be repeated the procedure during the lifetime of the product, so that also ageing effects are included in the digital twin. The parameters in the drivetrain digital twin, listed in TABLE I along with their datasheet/reference values, will be re-identified based on real experimental data. The other parameters described in section III are set as constant.

An approach is required for identifying the parameters, using the measurement data of quantities shown in Fig. 4. The identification approach uses the component models explained in section III and an optimization algorithm to fit the parameter values for a given load profile.

TABLE I
Parameters for Identification in the Drivetrain; the Datasheet Values Will Be Re-Identified Based on Load Cycle Measurements

Component	**Parameters**	**Datasheet/reference value**
Power Electronics	Switching loss factor	0.023 W/rpm
	Voltage drop factor	1.9V
	On-resistance factor	0.026 Ω
	Modulation factor (-)	-
Electric Motor	Winding resistance (phase), R_s	0.024 Ω
	d-axis inductance, L_d	0.002 H
	q-axis inductance, L_q	0.0044 H
	PM flux-linkage, λ_{PM}	0.2158 Wb
	Hysteresis loss factor, k_h	200
	Eddy current loss factor, k_c	0.1
Gearbox	Meshing constant	0.013
	Seal torque coefficient	-

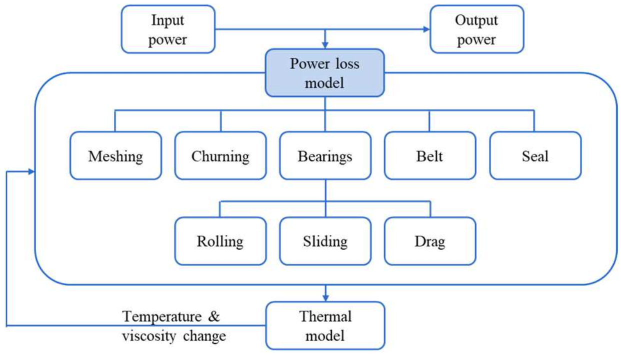

Fig. 7. Coupled power loss and thermal models.

The procedure aims to fit the calculated power of each component to the measured power in the several load profiles. The used cost function is given by (18).

$$f = min\left(\int_0^t P_{\text{in\_exp}} dt - \int_0^t P_{\text{in\_simulation}} dt\right) \tag{18}$$

t represents the time of the load cycle. $P_{\text{in\_exp}}$ represents the input power of the drivetrain over a complete load cycle in the time domain, while $P_{\text{in\_simulation}}$ denotes the input power of the drivetrain as computed by the digital twin for the same load cycle. It is important to note that for the digital twin, the output power of the drivetrain serves as the input. The digital twin then calculates the corresponding input power based on this output, reflecting the vehicle behaviour where the input power is provided as per the vehicle's mass and speed.

We consider the entire energy consumption of the load cycle. To find the optimal parameters, 1000 iterations are performed. modeFRONTIER software is used for the optimization, in which built-in pilOPT algorithm is utilized, which is a multi-strategy, self-adapting algorithm that combines the advantages of both local and global search strategies. This algorithm intelligently balances real and response surface methodology (RSM)-based (virtual) optimization to effectively search for the Pareto front.

The process for creating the digital twin is depicted in Fig. 8. Initially, a datasheet model based on the component models outlined in Section III is prepared, and the experimental data are imported into the MATLAB workspace. Subsequently, the MATLAB codes, Simulink models, and optimization software are configured to communicate with each other.

The next step involves selecting the bounds for the digital twin parameters within the optimization software. These parameters are iteratively optimized using an optimization algorithm. The process continues until the objective function

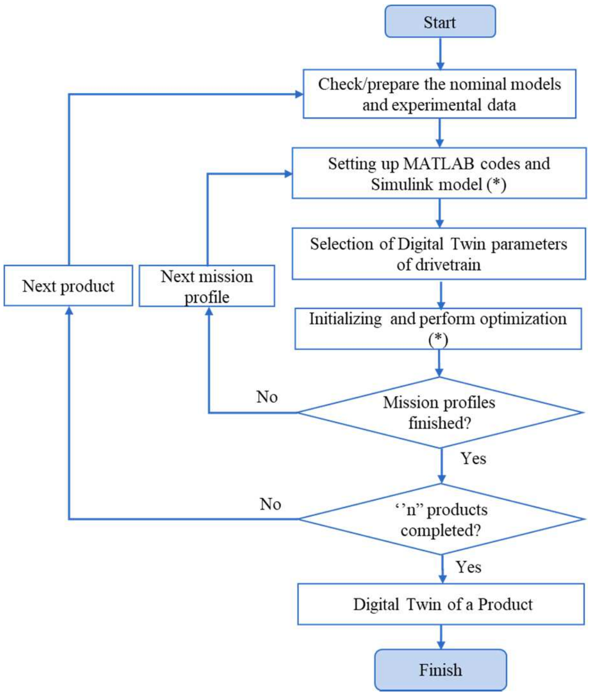

Fig. 8. The process for developing a digital twin

is minimized, at which point the final digital twin and the corresponding actual circuit parameters are obtained.

Once the procedure is performed for one load profile, then it will be repeated for the total number of load profiles of a single physical product. When the process is completed for one product, it can be applied to another product. However, the scope of this article is limited to the data from a single physical product, as discussed.

A. Concept of stochastic digital twin

The above described digital twin (DT) is extended to be a stochastic digital twin, where parameters are identified for all separate m number of load cycles. In other words, the parameters for the entire drivetrain, as specified in Table I, undergo fitting across m load profiles that are executed on a single physical product.

By using all those fitted values for each parameter and assuming a normal distribution of these values, the average and standard deviation of each parameter are computed. As an example, Eq. (19) and (20) illustrate the average and standard deviation of the phase winding resistance R_s of the motor, which is also depicted in Fig. 9. Next, the mean value of the fitted parameters is employed in constructing the ultimate digital twin for the corresponding physical product. This model is then utilized to predict the outcomes for a new load profile.

$$\mu_R = \frac{1}{m}\sum_{i=1}^{m} R_{s,i} \tag{19}$$

$$\sigma_R = \sqrt{\frac{1}{m}\sum_{i=1}^{m}(R_{s,i} - \mu_R)^2} \tag{20}$$

The digital twin is extended to be a stochastic digital twin in order to average out shortcomings of the model. Examples of shortcomings are unmodeled behavior of friction in motor bearings, temperature effects in the components, small eccentricities in the motor or gearbox. Although resistance of a winding can be measured as a deterministic value, the digital twin uses the stochastic version (19-20) to account for

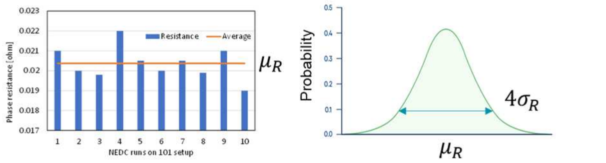

Fig. 9. Concept of stochastic digital twin: Gaussian distribution of the fitted phase winding resistance R_s.

e.g. unknown and changing temperatures, which may not be available from the field data of the motor.

V. Experimental Setup

An experimental setup is built to emulate different load profiles. The schematic of the drivetrain setup is shown in Fig. 10, and the details of the components are provided in TABLE II. The power electronics (PE) include two high performance AC drives, one for each motor. The two drives are directly connected through a DC-link, which allows to recirculate electrical energy from the generator (load motor) to the drive motor. Each drive powers and controls a single motor. The drive motor is a PMSM of 11kW. The load motor is an induction machine of 15kW: see TABLE II. The drive motor is connected to an industrial gearbox with helical gears. Lastly, a timing belt connects the gearbox to the load motor, which emulates a vehicle.

TABLE II

Component Specifications

Component	Description
PE drive motor	Nidec Unidrive M700 18.5 kW
PE load motor	Nidec Unidrive M700 18.5 kW
Drive motor	WEG W22 Magnet IE4, 11kW
Load motor	WEG W22 induction motor IE3, 15kW
Gearbox	Tramec ZA80B10, ratio 10.2:1
Timing belt	Optibelt 1696 8MHP50 ratio 3:1

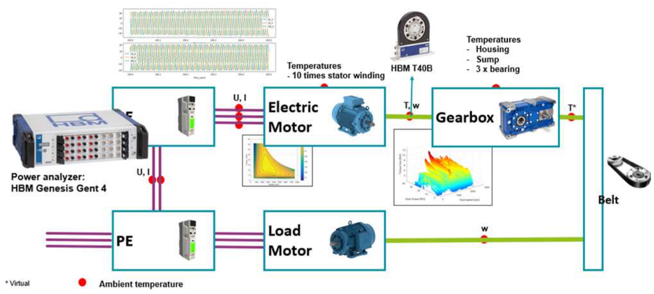

Fig. 10. Schematic of the drivetrain.

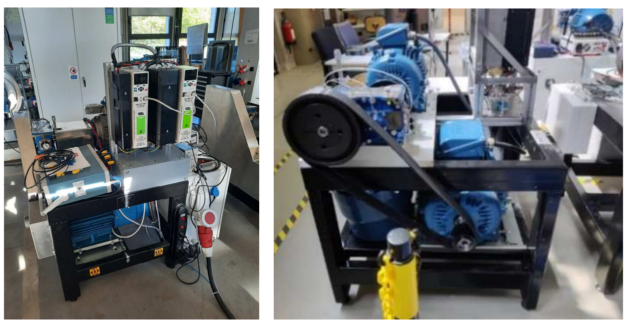

Fig. 11. One of the 5 test setups showing the drives and power analyzer (left figure) and the drive motor and gearbox at the top, and load motor at the bottom (right figure).

Five identical setups were built in order to create the stochastic digital twin for each of them, and in addition create a "fleet" digital twin of the whole fleet. The fleet digital twin is also a stochastic digital twin. This paper considers only data from 1 setup (MP-A1); results for the fleet digital twin based on 5 setups will be reported in future work. The motion product (MP-A1) is shown in Fig. 11.

VI. Results on Existing Load Profiles and the Evaluation of the New Load Profile

The load profiles for which we identified the digital twin parameters, are a torque staircase, given in Fig. 12-(a) and the new European driving cycle (NEDC), shown in Fig. 12-(b). One torque staircase load profile and 4 NEDC load profiles are measured on MP-A1 setup and data are used for the creation of the DT of the drivetrain. The approach explained in Fig. 8 is applied to identify all of the drivetrain's parameter values.

As we used five load profiles, we obtain m=5 values for each parameter. From these 5 values, the stochastic digital twin parameters are obtained, e.g. as in (19) and (20). As a showcase, two fitted parameter values of the drivetrain component (power electronics) are given in Fig. 13. The average values of the parameters are clearly seen from the figure. For the other fitted parameters, mean and standard deviation values are given in TABLE III.

We can now evaluate how good this stochastic digital twin is. Fig. 14 shows the efficiencies obtained in the 4 measured NEDC cycles, efficiency computed by the datasheet values based model and efficiency computed by the stochastic digital twin. It is clearly seen from the figure that the DT gives a better prediction than the datasheet based model. Note that Fig. 14 is not yet a virtual validation, because it shows results of the DT for the load profile that it was trained with. The aim of the DT is to show the prediction performance for a new load profile that was not used for training. This is done in the next paragraph.

As a new load profile, not used for training, the Worldwide harmonized Light Vehicle Test Procedure (WLPT) is selected.

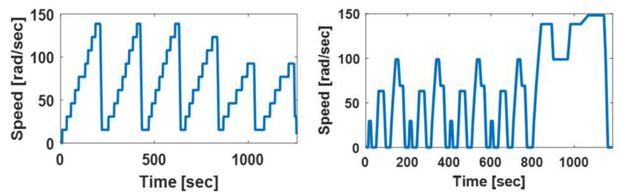

(a) (b)

Fig. 12. (a) Torque staircase (b) NEDC load profiles.

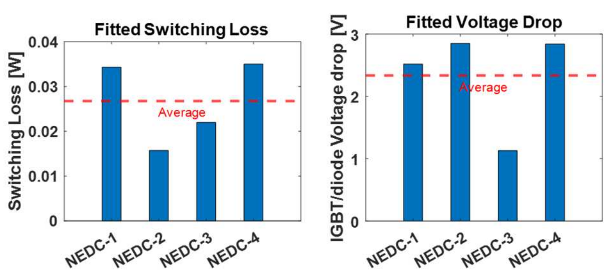

Fig. 13. Parameter identification results for power electronics using 1 torque staircase dataset and 4 NEDC datasets.

TABLE III
FITTED PARAMETERS OF THE DRIVETRAIN

Component	Parameters	Mean Value	Standard Deviation
Power Electronics	Switching loss factor	0.0267	0.00947
	Voltage drop factor	2.335	0.8178
	IGBT/diode on-resistance (Ω)	0.0325	0.0055
	Modulation factor (-)	0.0018	0.0012
Electric Motor	Winding resistance (phase), R_s	0.0215	0.0104
	q-axis inductance, L_q	0.00407	0.00218
	d-axis inductance, L_d	0.00195	0.0009
	PM flux-linkage, λ_{PM}	0.17237	0.0208
	Hysteresis loss factor, k_h	235.75	49.36
	Eddy current loss factor, k_c	0.3395	0.1135
Gearbox	Meshing constant	0.0258	0.0122
	Seal torque coefficient	0.38515	0.1977

The digital twin – trained by staircase and NEDC cycles data – is now run for the WLTP. To evaluate how good the DT performs, 4 WLTP cycles are also run experimentally. All results are compared in Fig. 15. It is observed that the datasheet model prediction overestimates the efficiency, while the DT prediction is well aligned with the experiments. Note that the blue measurements data were not used in digital twin creation, in order to get a virtual validation.

The Fig. 14 and Fig. 15 give the comparison of load cycles by taking the overall efficiency. It is better to have a close look to one of the load cycles in the time domain. The comparison of input power and losses from the experiment and the digital twin prediction for WLTP load cycles is shown in Fig. 16a and Fig. 16b. Fig. 16a illustrates the input power of the drivetrain, both measured directly and obtained from the digital twin. The experimental losses are computed via measured input and output power of the drivetrain. The same approach is performed in the digital twin, results are compared in Fig. 16b. It can be observed that the digital twin prediction of WLTP is well matched with experiment.

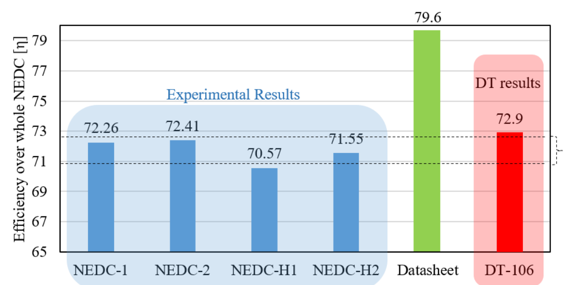

Fig. 14. Efficiency of the NEDC drive cycles; using datasheet values (green), measurements on the 4 setups (blue), and the digital twin predicted average (red). The blue measurement results were used to identify the digital twin, hence the red prediction is not a virtual validation.

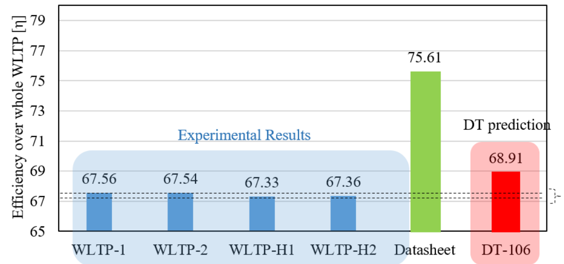

Fig. 15. Efficiency of the WLTP drive cycle; using datasheet values (green), measurements on the 4 setups (blue), and the digital twin predicted average (red).

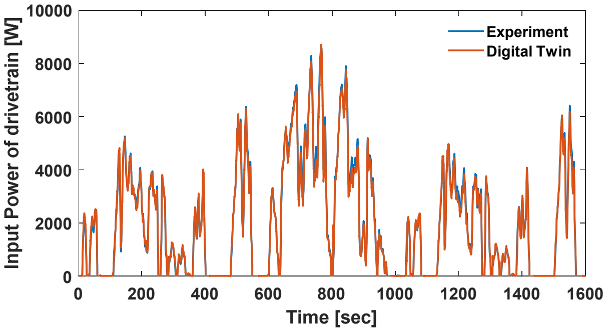

(a)

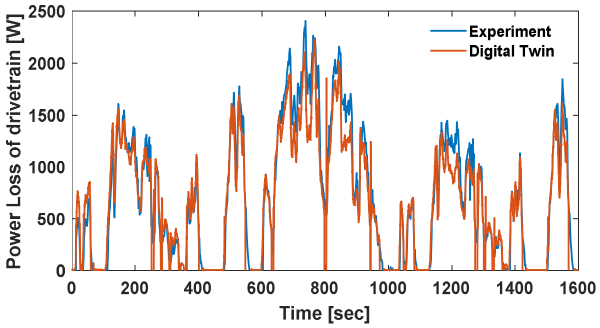

(b)

Fig. 16. Experiment and digital twin comparison for WLTP. (a) Input power of drivetrain (b) Experimentally computed (measured P_{in}-P_{out}) and the digital twin prediction of the losses.

VII. Similarity analysis of virtual prediction

For measured load profiles, i.e. profiles for which data are available, a similarity analysis is done to compare the digital twin prediction with measurements, and assess how similar they are. Equation (21) is employed to quantify the similarity between the output of the digital twin and experimental data.

$$S = \left(1 - \left|\frac{P_{L-DT}}{max_{1\leq i\leq N}\{P_{L-exp}\}} - \frac{P_{L-exp}}{max_{1\leq i\leq N}\{P_{L-exp}\}}\right|\right) * 100 \quad (21)$$

Here $P_{L\text{-}DT}$ and $P_{L\text{-}exp}$ represent the losses from the digital twin and from experiments as function of time, i.e. at each of the N number of points in the load profile. Note that S is also a time series of N points.

The similarity assessment for the WLTP cycle is given in Fig. 17. The scatter plot illustrates the degree of similarity between the experimental data and the Digital Twin output across all speed points of the WLTP cycle within the time domain. It is clear that there is a strong similarity between the digital twin and the experimental results. This indicates that the proposed digital twin has good accuracy in predicting the efficiency of new load profiles.

If the similarity is not sufficient in certain regions of the load profile, the digital twin can be improved by adding unmodelled behavior. However, this is beyond the scope of this article.

VIII. Conclusion

In this paper, a digital twin of complete drivetrain is developed. It is capable of performing virtual validation of load profiles that have not been previously tested. The output of the digital twin for a new load profile is verified by experimental test and similarity analysis. The presented digital twin is developed based on one physical product.

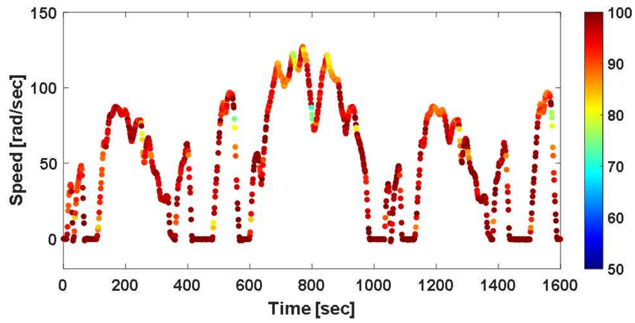

Fig. 17. The similarity between outcomes from the digital twin and experimental loss results during the WLTP cycle.

In the future, we will extend this approach to multiple drivetrain products. For this, four additional identical drivetrains have been built to gather data and create a fleet digital twin.

ACKNOWLEDGMENT: This research is financially supported by Flanders Make SBO project DT for Validation of Dynamic Performance & Reliability of Motion Systems.

IX. References

[1] F. Tao, H. Zhang, A. Liu and A. Y. C. Nee, "Digital Twin in Industry: State-of-the-Art," in IEEE Transactions on Industrial Informatics, vol. 15, no. 4, pp. 2405-2415, April 2019.

[2] M. Ibrahim, V. Rjabtšikov, S. Jegorov, A. Rassõlkin, T. Vaimann and A. Kallaste, "Conceptual Modelling of an EV-Permanent Magnet Synchronous Motor Digital Twin," 2022 IEEE 20th International Power Electronics and Motion Control Conference (PEMC), Brasov, Romania, 2022.

[3] Z. Chen, D. Liang, S. Jia, L. Yang and S. Yang, "Incipient Interturn Short-Circuit Fault Diagnosis of Permanent Magnet Synchronous Motors Based on the Data-Driven Digital Twin Model," in IEEE Journal of Emerging and Selected Topics in Power Electronics, vol. 11, no. 3, pp. 3514-3524, June 2023

[4] A. Rassõlkin et al., "Interface Development for Digital Twin of an Electric Motor Based on Empirical Performance Model," in IEEE Access, vol. 10, pp. 15635-15643, 2022.

[5] B. Rodríguez, E. Sanjurjo, M. Tranchero, C. Romano, and F. González, "Thermal parameter and state estimation for digital twins of E-powertrain Components," IEEE Access, vol. 9, pp. 97384-97400, 2021.

[6] W. Song, Y. Zou, C. Ma and S. Zhang, "Digital Twin Modeling Method of Three-Phase Inverter-Driven PMSM Systems for Parameter Estimation," in IEEE Transactions on Power Electronics, vol. 39, no. 2, pp. 2360-2371, Feb. 2024.

[7] K. Yamazaki and N. Fukushima, "Iron-Loss Modeling for Rotating Machines: Comparison Between Bertotti's Three-Term Expression and 3-D Eddy-Current Analysis," in IEEE Transactions on Magnetics, vol. 46, no. 8, pp. 3121-3124, Aug. 2010.

[8] Benedict GH, Kelley BW. Instantaneous coefficients of gear tooth friction. ASLE transactions, 4(1):59-70, 1961.

[9] Zhu B, Wang X, Luo L, Zhang N, Liu X. Influence of lubricant supply on thermal and efficient performances of a gear reducer for electric vehicles. Journal of Tribology, 144(1), 011202, 2022.

[10] Harris TA, Kotzalas MN. Essential concepts of bearing technology, CRC press, 2006.

[11] SKF Group, SKF general catalogue, 2008.

[12] M. Zadeh Fard, A., Vanpaemel, S., Janssens, D., Kirchner, M., Laurijssen, K., Divens, N., Claeys, C., Pluymers, B., Naets, F. (2023). Assessing the accuracy of a thermo-mechanical model of a gearbox. In: 4th Future of Road Mobility Forum - FORM Forum scientific proceedings, (17-22).